Materiales de Construcción
Vol. 64, Issue 313, January–March 2014, e007
ISSN-L: 0465-2746
http://dx.doi.org/10.3989/mc.2014.01513

Experimental study of masonry wall exposed to blast loading

S. Ahmad[a], A. Elahi[a], H. Pervaiz[a], A.G.A. Rahman[b], S. Barbhuiya[c]✉

a. University of Engineering and Technology (Taxila, Pakistan)
b. University of Malaysia (Pahang, Malaysia)
c. Curtin University of Technology (Perth, Australia)
✉Salim.Barbhuiya@curtin.edu.au

Received 13 February 2013
Accepted 10 July 2013
Available on line 18 March 2014

ABSTRACT: The challenge of protecting the nation against the attack of terrorism has raised the importance to explore the understanding of building materials against the explosion. Unlike most of the building materials, brick masonry materials offer relatively small resistance against blast loading. In this research, a brick masonry wall was exposed to varying blast load at different scaled distances. Six tests with different amounts of explosives at various distances were carried out. Pressure time history, acceleration time history and strain at specific location were measured. The parameters measured from experimental pressure time history and acceleration time history is compared with those determined by ConWep to establish the correlations between experimental determined records and ConWep values. The experimental results were also compared with some researchers. These correlations may assist in understanding the behaviour of masonry structures subjected to explosive loading.

KEYWORDS: Brick; Acceleration; Deformation; Compressive strength

Citation / Citar como: Ahmad, S.; Elahi, A.; Pervaiz, H.; Rahman, A.G.A.; Barbhuiya, S. (2014). Experimental study of masonry wall exposed to blast loading. *Mater. Construcc.* 64 [313], e007 http://dx.doi.org/10.3989/mc.2014.01513

RESUMEN: *Estudio experimental del comportamiento de una fábrica sometida a cargas explosivas.*- Con el reto que supone proteger a la nación contra atentados terroristas se ha visto acrecentada la importancia de conocer el comportamiento de materiales de construcción cuando se someten a una carga explosiva. Al contrario de la mayoría de los materiales, las fábricas de ladrillo ofrecen poca resistencia a dichas cargas. En el presente trabajo, se estudió el comportamiento de una fábrica de ladrillo ante cargas explosivas colocadas a diferentes distancias del muro. Se realizaron seis pruebas con explosivos de potencias distintas y a diferentes distancias. Se trazaron las curvas presión-tiempo y aceleración-tiempo, midiéndose asimismo la deformación en un punto concreto. Los valores experimentales de las curvas presión-tiempo y aceleración-tiempo se compararon con los que se calcularon con la ayuda de la aplicación informática ConWep a fin de establecer las correlaciones entre ambos conjuntos de resultados. También se compararon los resultados experimentales obtenidos con los publicados por otros investigadores. Estas correlaciones podrían contribuir a mejorar el conocimiento del comportamiento de estructuras de fábrica sometidas a cargas explosivas.

PALABRAS CLAVE: Ladrillo; Aceleración; Deformación; Resistencia a la compresión

1. INTRODUCTION

The threat of terrorism has increased the need for engineers to have confidence that buildings can withstand the significant loads experienced during a blast event. The destruction of load bearing masonry walls can lead to the more serious problem of progressive collapse, it is therefore important that behaviour of masonry structure must be known in order to take special measures to avoid structural failure. Masonry walls are generally used in almost all types of building construction in different parts

of the world and have considerable historical and architectural worth. Masonry walls have many advantages such as easy availability, low cost building material, and excellent sound and insulation properties. Under blast loading, masonry walls exhibit brittle behaviour. Failure of a masonry wall is likely to be sudden and severe that pose significant debris hazard to building occupants when subjected to blast loads (1, 2). Based on field test observations, the damages on the wall were classified in four levels by Varma et al. (3). Blast explosions generate pressures of high intensity and short duration. These extreme forces cause enormous displacement deformation and the resulting breakage of nearby objects. The term of explosion means a large scale, sudden and rapid release of the energy in an extreme manner followed by pressure wave propagation. The mutual interactions of the air and obstacles at the interface will decide the structural response, damage and fracture. Retrofitting of wall is a practical way of reducing the susceptibility to blast loading, thereby, mitigating danger to occupants in the occurrence of an external explosion (1). Different studies have raised different parameters to strengthen masonry wall against such an extreme loading cases (4, 5). The pressure impulse curves defining different damage areas have been extensively used for assessing the damage of masonry walls and other structural components subjected to blast loads (6).

Behavior of structures when subjected to both air blast and ground shock pressure waves from surface explosion were studied by Wu & Hao (7). One story masonry in-filled reinforced concrete frame was considered in the investigation. Dynamic response of the structures to the pressure forces was then calculated. It was concluded that air blast load dominates structural response and damage for small scaled distances, whereas, ground shock pressure governs surface explosion at large scaled distance. Also it was investigated that at large scaled distance, ground shock and air blast force can be evaluated separately as the effects of both on structures decoupled. It was further concluded that structural damage would be seriously underestimated if ground shock were neglected under certain conditions. Godinho et al. (8) studied resistance of unreinforced masonry walls to air blast loads. Authors demonstrated that the wall would have undergone out-of-plane flexure and produced tensile strains on the inner face of the wall and compressive strains on the exterior face when encountered to an air blast load. The wall, then would have gone through negative deflection developing tensile strains on the exterior face of the wall and amplifying shear stresses at wall supports. So it was suggested that exterior masonry walls should be made stronger with glazed elements. As the breakage of these elements release some blast pressure, this reduces the effect of blast load forces on the remaining structure.

Analysis and design of structures under blast explosion require a detail understanding of blast phenomenon and dynamic response of structural elements. Ngo et al. (9) discussed nature of explosions, blast wave propagation in air and different techniques used to predict the response of structure when detonated. It was highly recommended to use technical design manuals in current building design codes to prevent structure vulnerability and progressive collapse. Urgessa (10) conducted a blast test on eight masonry walls retrofitted with fibre reinforced polymer. These walls were exposed to blast loads of 0.45 kg. Pressure time history and displacement response of the structure were measured. Measured blast wave parameters were observed to be in a good agreement with parameters determined from Single-Degree-of-Freedom (SDOF) dynamic analysis.

In another study, numerical simulations on LS DYNA were carried out for the assessment of the response of unreinforced brick masonry walls exposed to blast loading (11). The effects of material strength, boundary conditions and thickness of the wall under blast loads were studied. It was concluded that there was a marginal effect of mortar and brick strength on the structural response under larger detonation. Thickness of the wall was observed to be a dominating parameter in producing considerable effect on the response and damage of masonry walls. Different types of boundary conditions of the wall were taken into consideration. It was found that the boundary condition has a remarkable effect on the response and failure of the walls.

In a recent study, effect of variety of commonly used material was examined from existing literature on blast loading (12). This study is an important tool to blast investigators in order to understand the effect of size and location of the blast explosive from the target. Five conventional buildings were reviewed in terms of observed damage on the material after blasting. Most of the research has been undertaken in the field of dynamic analysis for the modeling of blast pressure on the structures (13, 14, 15). The present results allow a detailed study of the simultaneous air blast pressure and ground shock on structures. Unreinforced masonry walls are commonly susceptible to out-of-plane loads. It is, thus, of interest to understand the behavior of unreinforced masonry walls under blast loading. The current research work will contribute in understanding the behaviour of masonry wall against explosion loads.

2. EXPERIMENTAL PROGRAMME

2.1. Experimental Scheme

A masonry wall of 2 m×2 m was constructed. A scheme of wall is shown in Figure 1. The wall was then exposed to varying blast loads. Six tests with different amounts of explosives were carried out. Quantity of charge was varied from 4 kg to 14 kg with

FIGURE 1. View of brick masonry wall.

an increment of 2 kg. Distance of explosive location to the target centre varies from 3 m to 4 m respectively. Nitroglycerin based dynamite explosive was used. Vertical wooden support was erected to hold charge mass 1m above the ground. This whole work had been carried out in hilly area of Hassan-Abdal (Punjab), Pakistan. TNT equivalent of nitroglycerin dynamite explosive is 0.6. It is customary to refer the weight of explosives used in experimental tests to an equivalent weight of TNT. Formby & Wharton (16) offered results to obtain TNT equivalency of various commercial explosives. Material properties of brick are given in Table 1. Experimental data of six tests with different standoff distance and amount of explosive used is given in Table 2.

2.2. Measuring devices and explosive charge

Different measuring instruments were installed to record pressure, acceleration and strains at a given locations over time during the test. Measurement devices give strain, pressure time history and acceleration time history; an important element concerning response of structures to air blast loading. These

TABLE 1. Material properties of brick

Constructive element	Density ρ (kg/m^3)	Compressive strength f_c (MPa)	Young's Modulus E (MPa)	Poisson's ratio ν
Solid clay brick	1800	6.76	6084	0.17

TABLE 2. Experimental data

BRICK MASONRY WALL (2 m×2 m×0.381 m)			
Charge mass, Q (kg)	**TNT Equivalent Weight, Q_{TNT} (kg)**	**Stand-off distance, R (m)**	**Scaled distance $Z=R/Q^{1/3}$ [m/(kg$^{1/3}$)]**
4	2.4	3	2.24
6	3.6	3.5	2.28
8	4.8	3.5	2.07
10	6	4	2.20
12	7.2	3.5	1.81
14	8.4	3.5	1.72

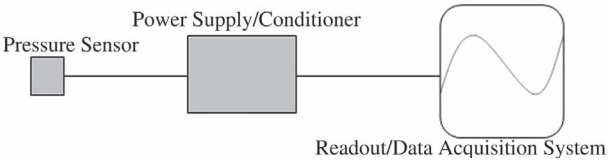

FIGURE 2. Scheme of Pressure sensor.

parameters were measured using pressure sensors, accelerometer and data acquisition system. For better understanding of the complex dynamic response, high-speed camera was used. Different measuring devices were employed to monitor the response of masonry wall to the blast loading. PCB Sensors of 200 psi range was used in current blast wall pressure measurement to measure the overpressure generated by shock waves. This sensor was placed at the center of the wall exposed to impulsive loading as shown in Figure 2. PCB pressure sensor is Integrated-Circuit Piezoelectric (ICP) voltage mode sensor. This converts input pressure to high-resolution curve that is virtually insensitive to length of cable. It was connected to the data acquisition system module shown in Figure 2.

In order to measure dynamic response of wall in three mutually perpendicular axes, triaxial accelerometer was used in blasting on brick masonry wall. It was fixed at the center and on backside of concrete wall using adhesive as shown in Figure 3. After preparation of the surface, the strain gauges were glued at the centre of the masonry wall as

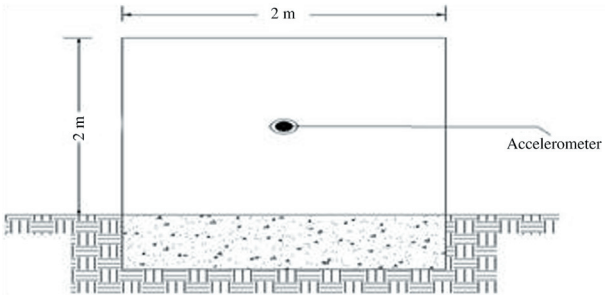

FIGURE 3. Location of Accelerometer (Backside of wall).

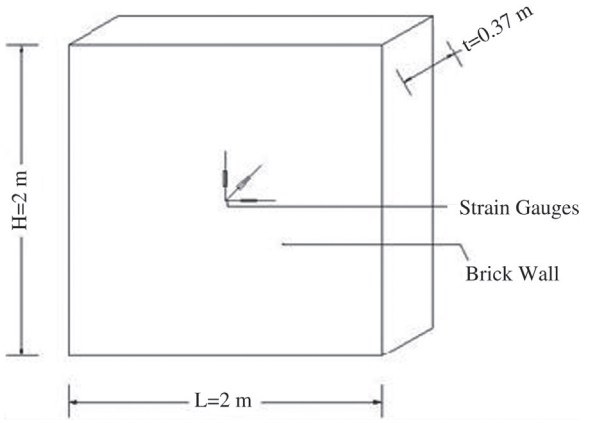

FIGURE 4. Location for strain gauge installation.

FIGURE 5. High-speed camera images of blast wave propagation.

shown in the Figure 4. Strain gauges were connected to Strain Indicator and Recorder. It has four input channels. LCD display of the equipment readout the strain.

In addition a data acquisition instruments was used. It was mounted on a computer that record and process the signals by means of a computer program. It has 16 input channels, 2 output channels and has a capacity of 200 KS/s (Kilo Sample/Second) and16-bit Multifunction I/O. Nitroglycerin Based Dynamites was used in this experiment of blasting operation. In this test, it is used in 80% in mass of TNT. Images of blast explosion captured by high-speed camera are shown in Figure 5.

Figure 6 shows the damage pattern of detonated masonry wall. It can be noted that when the quantity of explosive was 6 kg, insignificant cracks were observed. Masonry wall still maintains the integrity as before. With the increase in the quantity of the explosive, several cracks along the longitudinal direction were noticed. Depth of cracks grows with increasing the quantity of explosive. Under the explosive load of 12 kg, a large longitudinal crack along the front and back side of the wall was noticed. It was observed that masonry wall suffered from a non-repairable damage. For 14 kg explosive load, the wall fall down along the weak plane i.e. along longitudinal crack.

3. RESULTS AND DISCUSSION

The brick wall collapsed in the field at 14 kg explosive load. The results from all six tests are presented below:

3.1. Pressure time history

Records of the time histories of the overpressure that was measured at the centre of brick wall are shown in Figures 7 and 8. Pressure wave follows the classical shape of pressure time history.

3.2. Acceleration time history

The accelerations that were measured in all three directions at the centre of the wall are shown in Figures 9 and 10. The obtained value of acceleration has a connection with the damage/failure pattern of the specimen.

3.3. Experimental results of strain

The time dependent strains that were measured at the center of the brick wall are shown in Figure 11. 45° strain rosette was used. It is clearly seen that peak strain for 12 kg explosion was greater than six explosive loads.

(a) 6 kg (b) 12 kg

FIGURE 6. Blast loaded wall after explosion.

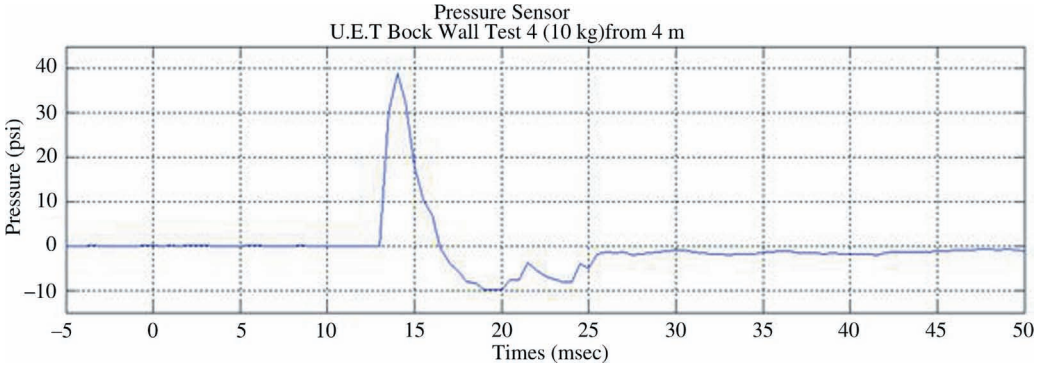

FIGURE 7. Measured pressure-time history of 10 kg surface explosion (4 m from charge centre).

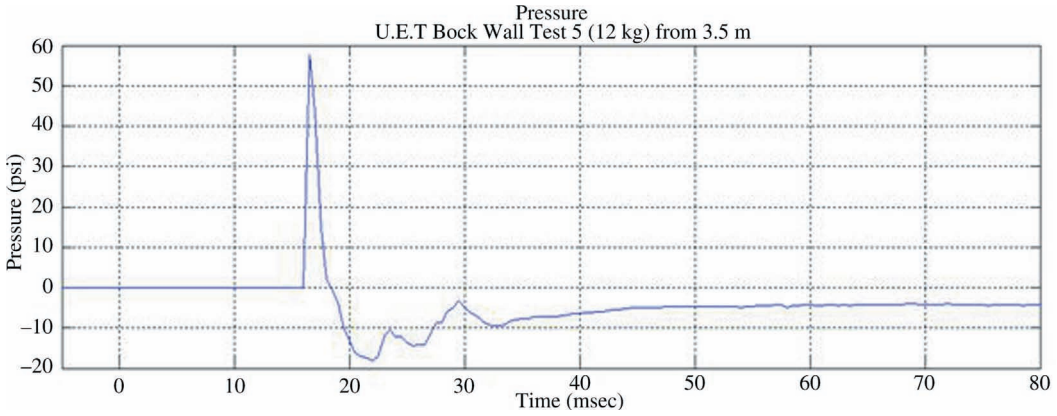

FIGURE 8. Measured pressure-time history of 12 kg surface explosion (3.5 m from charge centre).

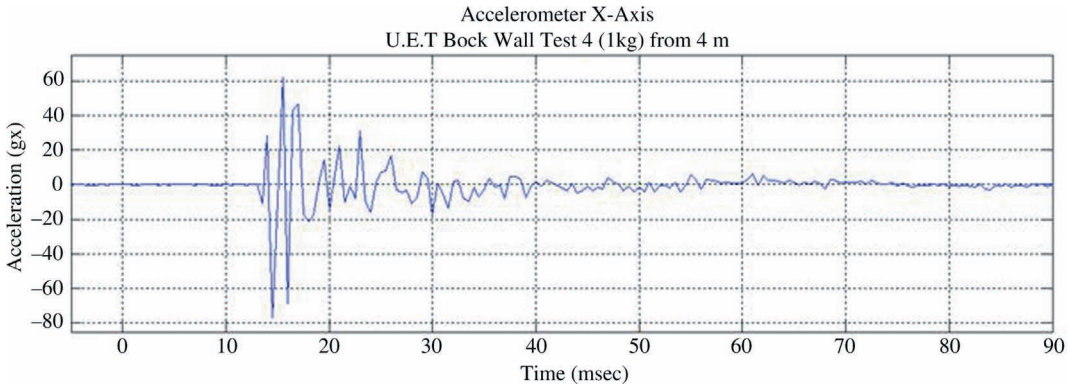

FIGURE 9. Acceleration time history (g_x) of 10 kg surface explosion (4 m from charge centre).

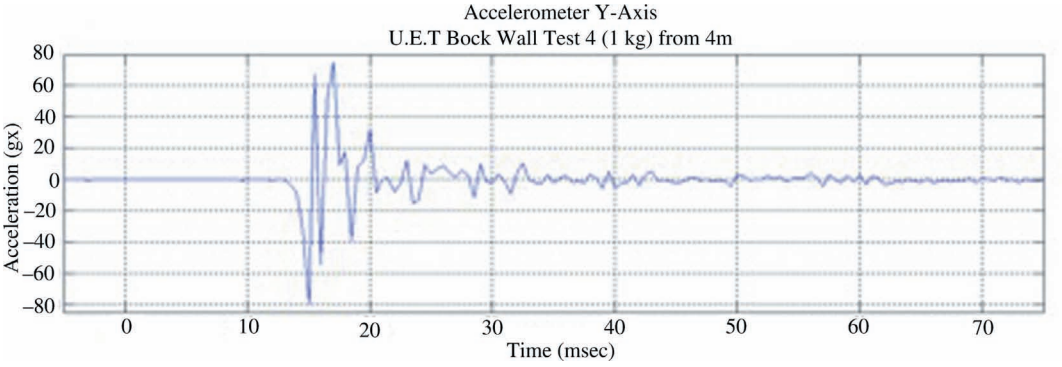

FIGURE 10. Acceleration time history (g_y) of 10 kg surface explosion, 4 m from charge centre.

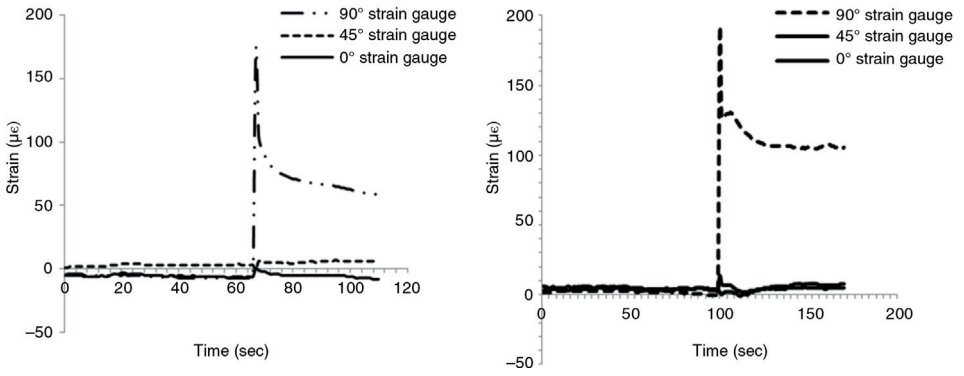

FIGURE 11. Strain vs. time of brick wall under explosive load.

Table 3. Experimental values of air blast wave parameters

Scaled distance (m/kg$^{1/3}$)	AIR BLAST WAVE PARAMETERS					
	P_{so} (MPa)					
	Experimental	TM-5	T_a (sec)	T_r (sec)	T_d (sec)	T (sec)
1.72	0.6115	0.5502	0.01301	0.00088	0.00179	0.00267
1.81	0.4099	0.4791	0.0159	0.00067	0.00173	0.0024
2.07	0.2776	0.339	0.012	0.00155	0.0022	0.00375
2.20	0.2692	0.3357	0.01298	0.00114	0.00253	0.00367
2.24	0.2158	0.2654	0.01099	0.00052	0.003115	0.00364
2.28	0.2075	0.275	0.01	0.00049	0.00331	0.0038

Table 4. Comparison of experimental peak pressure with ConWep and other published work

Scaled distance (m/kg$^{1/3}$)	P_{so} (MPa)			
	Experimental	ConWep	UFC	AASTP
1.72	0.6115	0.489612	0.5502	0.57
1.81	0.4099	0.432874	0.4791	0.43
2.07	0.2776	0.31285	0.339	0.258
2.20	0.2692	0.277346	0.3357	0.224
2.24	0.2158	0.251838	0.2654	0.216
2.28	0.2075	0.248598	0.275	0.2062

3.4. Comparison with predicted values

Comparison of calculated parameters with ConWep (17) is done to check correlation between experimental determined records and ConWep values. The present results allow a detailed study of the simultaneous airblast pressure and ground shock on structures.

3.4.1. Air blast wave parameters

Usually the air blast wave parameters are peak pressure P_{so}, arrival time T_a, rising time to the peak value of pressure T_r and decreasing time from peak to ambient pressure T_d and total duration of positive pressure phase of pressure time history are given in Table 3.

3.4.2. Peak air pressure

Using the experimental pressure time history, the peak value of incident overpressure is determined. Comparison between peak values of pressure determined by experimental pressure time data, ConWep calculated values, UFC (18) and AASTP (19) for hemispherical surface explosion along with their best fitted curve are reported in Table 4 and are further graphically shown in Figure 12. As shown, the experimental variation of peak pressure with scaled distance confirmed the results calculated by means of ConWep, UFC and AASTP chart for hemispherical surface explosion. Experimental results are comparatively more consistent with those as predicted by AASTP.

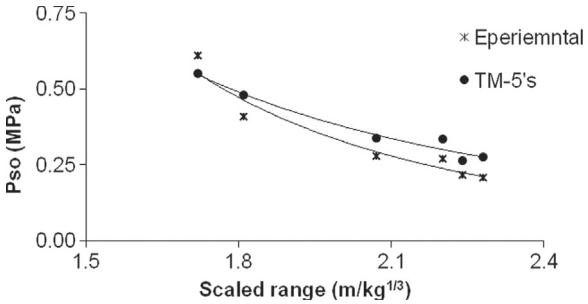

Figure 12. Relationship between peak pressure attenuation and standoff distances.

3.4.3. Comparison between empirical equations of P_{so}

Many empirical relationships are available in the literature for predicting peak overpressure attenuation against scaled ranges. Brode's (13, 20, 21) empirical formulae for peak pressure in an unlimited atmosphere are [1] [2]:

$$p_{so}=0.67\left(\frac{R}{Q^{1/3}}\right)^{1/3}+0.1,\ p_{so}>1\ (\text{MPa}) \qquad [1]$$

$$p_{so}=0.098\left(\frac{R}{Q^{1/3}}\right)^{-1}+0.1465\left(\frac{R}{Q^{1/3}}\right)^{-2}+0.585\left(\frac{R}{Q^{1/3}}\right)^{-3}-0.0019,\ 0.1\le p_{so}\le 1\ (\text{MPa}) \qquad [2]$$

Table 5. Comparison of Empirical Equations for P_{so}

Scaled Range ($m/kg^{1/3}$)	Current Research	Saeed et al. (2012)	Siddiqui & Ahmad (2007)	Wu and Hao (2005)	Brode (1955)	Hynrych and Major (1979)
1.72	0.533	0.578	0.361	0.338	0.219	0.3906
1.81	0.4466	0.505	0.327	0.3058	0.1956	0.3678
2.07	0.28	0.353	0.253	0.234	0.1456	0.3153
2.2	0.227	0.2997	0.226	0.2066	0.1278	0.2945
2.24	0.2132	0.286	0.218	0.1993	0.1231	0.2887
2.28	0.201	0.272	0.211	0.1923	0.1186	0.283

Wu nd Hao (22) determined peak pressure at the target points in the air using simulated pressure time histories at a hemispherical shock wave front is [3]:

$$p_{so}=0.059\left(\frac{R}{Q^{1/3}}\right)^{-2.56}-0.051, \quad 0.1\le (\mathrm{R}/\mathrm{Q})^{1/3}\le 1 \ \ (\mathrm{MPa}) \qquad [3]$$

Siddiqui and Ahmad (23) carried out research work on nuclear containment structure and found following empirical formula for peak pressure [4]:

$$p_{so}=1.017\left(\frac{R}{Q^{1/3}}\right)^{-1.91}, \ 12\ge (\mathrm{R}/\mathrm{Q})^{1/3}\ge 1 \ (\mathrm{MPa}) \qquad [4]$$

Experimental results by Ahmad et al. (24) have generated the following relationship of P_{so} with respect to the scaled distance [5]:

$$p_{so}=2.46\left(\frac{R}{Q^{1/3}}\right)^{-2.67} \ (\mathrm{MPa}) \qquad [5]$$

Whereas current research on brick masonry wall have suggested empirical attenuation relation for peak air pressure for a hemispherical shock wave front as under [6]:

$$p_{so}=3.495\left(\frac{R}{Q^{1/3}}\right)^{-3.408} \ (\mathrm{MPa}) \qquad [6]$$

Where R is standoff distance in meters measured from charge center and Q is TNT equivalent charge weight in kilograms. At different scaled distance peak air pressure determined by empirical formulae are given in Table 5.

Peak air pressures determined by present functions, by other empirical relations are then plotted in curves, expressed in Figure 13. As shown in Figure 13, for all scaled distances exponential decay of peak pressure of present research on brick wall are in close agreement with Siddiqui and Ahmad and Wu and Hao's results. Large variations of peak pressure are noticed with Henrych's curve. Brode (13)'s and Ahmad et al.'s derived relations show similar behavior but peak pressures are quite different.

3.4.4. Arrival time air blast wave

The shock wave front arrival time T_a is usually not included in the most of the studies on impulsive loading, are estimated here. Arrival time at different scaled distances is shown in Figure 14. As shown in this figure, with increasing scaled distance air blast wave arrival time decreases. Also it can be stated that at the same scaled distance, the smaller the explosive weight is, longer will be the arrival time. Empirical formula derived using experimental result for shock wave arrival time is [7]:

$$T_a=\frac{8.534}{C_a}\left(\frac{R}{Q^{1/3}}\right)^{-0.996} \ (\mathrm{s}) \qquad [7]$$

Where arrival time of air blast wave is in seconds, R is the standoff in meters, and Q is the TNT equivalent charge weight in kg. C_a is the velocity of sound in air, taken as 340 m/s. As shown in Figure 14, with increasing scaled distance air blast wave arrival time decreases. Also it can be stated that at the same scaled distance, the smaller the explosive weight is, longer will be the arrival time.

3.4.5. Rising time of shock wave

Rising time is defined as the time when pressure rises rapidly from ambient to peak pressure. In the literature, rising time is mostly not included as this time is very short. Pressure time wave is typically

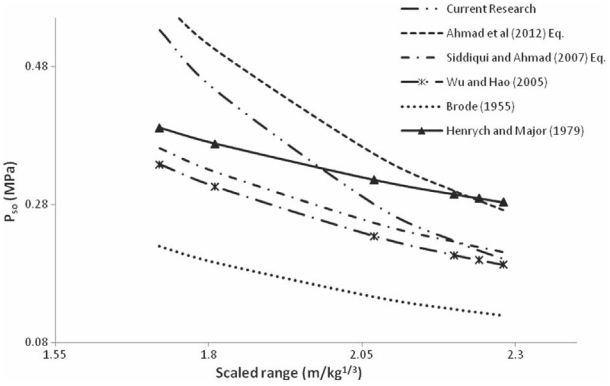

Figure 13. Graph showing comparison of empirical equations for P_{so}.

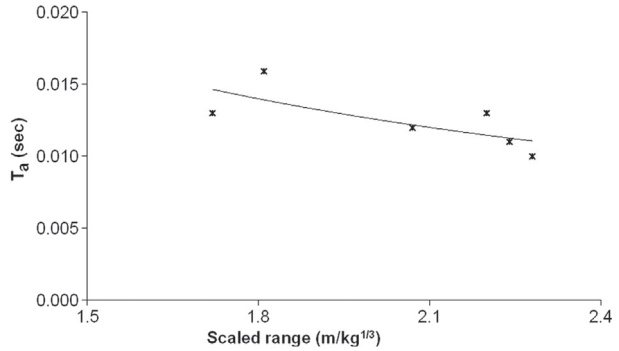

FIGURE 14. Arrival time of air blast wave against scaled distance.

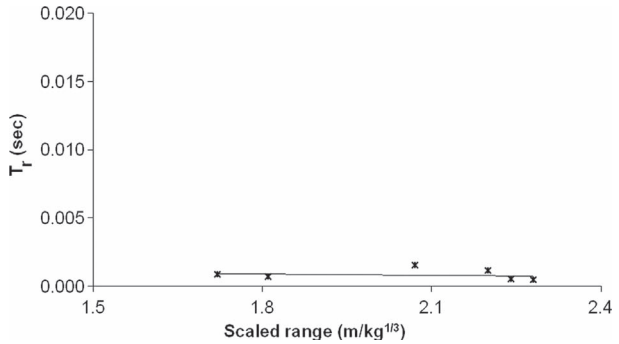

FIGURE 15. Rising time of air blast wave against scaled distance.

assumed starting from peak value and then exponentially decays to ambient value. For more accurate analysis of structures against blasting, rising time is considered in this study. Pressure increases exponentially from zero to peak value having a rising time T_r shown in Figure 15. Derived empirical relationship using experimental data for rising time of shock wave is [8]:

$$T_r = 0.0014\left(\frac{R}{Q^{1/3}}\right)^{-0.759} \text{ (s)} \qquad [8]$$

Where rising time is in seconds, R is the range in meters, and Q is the TNT equivalent charge weight in kg.

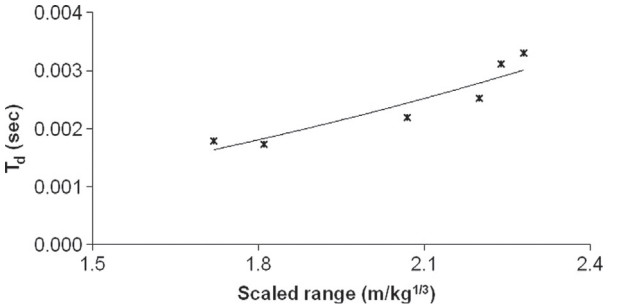

FIGURE 16. Decreasing time of air blast wave against scaled distance.

3.4.6. Decreasing time of air blast wave

Decreasing time is the time when pressure drops from peak to ambient value, another parameter for modeling of pressure time history shown in Figure 16. Based on experimental data the best-fitted relation is [9]:

$$T_d = 0.0005\left(\frac{R}{Q^{1/3}}\right)^{2.159} \text{ (s)} \qquad [9]$$

3.4.7. Positive phase duration of shock wave

Positive phase duration is the summation of rising time and decreasing time.

So it can be written as [10]:

$$T_+ = T_r + T_d \qquad [10]$$

Combining equation the positive phase duration is [11]:

$$T = 0.0014\left(\frac{R}{Q^{1/3}}\right)^{-0.759} + 0.0005\left(\frac{R}{Q^{1/3}}\right)^{2.159} \text{ (s)} \qquad [11]$$

Figure 17 is the graphical variation of positive phase duration against scaled distance.

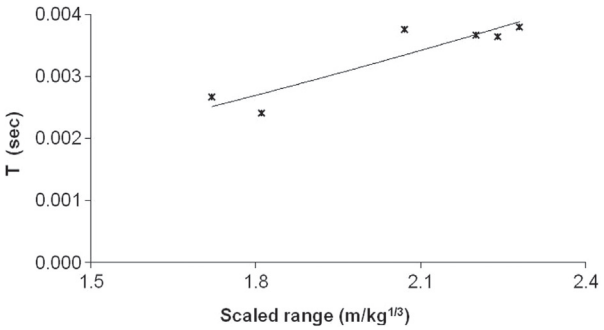

FIGURE 17. Positive phase duration against scaled distance.

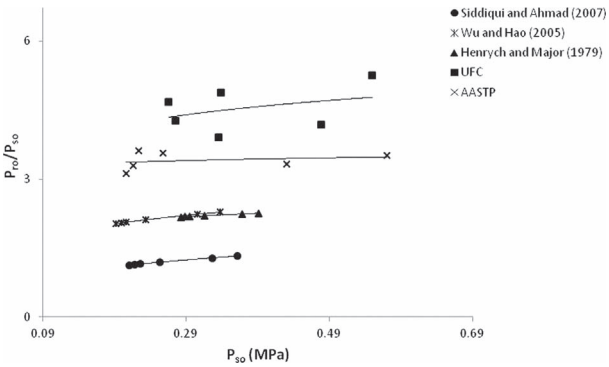

FIGURE 18. Ratio of horizontal peak reflected pressure to the peak air pressure against peak air pressure.

Table 6. Experimental values of ground shock wave parameters

Scaled distance ($m/kg^{1/3}$)	GROUND SHOCK WAVE PARAMETERS					
	PPA (m/s^2)		t_a (sec)		t_d (sec)	
	Experimental	ConWep	Experimental	ConWep	Experimental	ConWep
1.72	186.865	109.1	0.0121	0.01303	0.05721	0.04962
1.81	112.678	94.72	0.01725	0.01293	0.046112	0.04478
2.07	151.742	65.32	0.012	0.01206	0.04378	0.04211
2.20	76.945	50.23	0.0119	0.01352	0.03911	0.04191
2.24	125.404	58.65	0.0105	0.01037	0.03639	0.037
2.28	90.81	50.18	0.00875	0.01193	0.03182	0.03007

3.4.8. Peak reflected pressure

In air blast pressure time history, when incident wave impinges with the structure e.g. wall it will reflect. When the blast wave is reflected against the perpendicular surface, it may result in enhanced intensity reflected pressure as compared to incident pressure wave. Design manual, UFC (18) and AASTP (19) chart provide curves to calculate peak reflected pressure from the peak incident air pressure. Various relationships of reflected pressure are also available in literature relating peak reflected pressure to the peak free incident air pressure. Figure 18 shows comparison of UFC (18), AASTP (19) design manual with the empirical relationships of other researchers of peak reflected pressure and peak air pressure. As shown, that ratio increases with the increase in peak air pressure. Variation of design chart values with Siddiqui and Ahmad (23) is due to the curved concrete structure. Henrych and Major (14) and Wu and Hao (22) show small variation this may be attributed to the numerical simulation results of pressure.

3.5. Ground shock wave parameters

Ground shock wave history is defined by its peak value, time of arrival of ground shock waves; duration and time difference in arrival of air blast and ground shock waves given in Table 6. The Conwep software (17) has been used for comparison of various ground shock parameters with the experimental values. This program calculates the peak free-field stress owing to the directly transmitted shock wave, and optionally allows the addition of a reflected wave from a deeper layer and a relief (tension) wave reflected from the ground surface. It is important to note that relief wave effects for high magnitude shocks and/or near surface detonations are not well understood, and inclusion of a relief wave in these situations may lead to un-conservative answers. Peak particle velocity, acceleration and displacement are calculated using the direct path only. Reflections from the surface or a lower layer are not included.

3.5.1. Peak particle acceleration

Peak particle acceleration is the maximum acceleration of acceleration time history graph. Experimental and ConWep obtained PPA for different charge weights are shown in Figure 19. Empirical relation of PPA provides the surface ground motion as a function of scaled distance is [12]:

$$PPA = 421.18\left(\frac{R}{Q^{1/3}}\right)^{-1.774} \left(\mathrm{m/s^2}\right) \quad [12]$$

3.5.2. Ground shock wave arrival time

In modeling of simultaneous air blast and ground shock forces on structures, arrival time of ground shock motions is needed. Experimental values when plotted in Figure 20 gave the following empirical equations [13]:

$$t_a = \frac{46.17}{C_S}\left(\frac{R}{Q^{1/3}}\right)^{-1.32} \mathrm{(s)} \quad [13]$$

The soil possessed the following properties: Density=1920 kg/m^3, seismic velocity of the soil C_s=1524 m/sec.

3.5.3. Duration of ground shock wave

An important parameter that appreciably affects the structural response against impulsive loading is the duration of shock wave in Figure 21. Shock wave

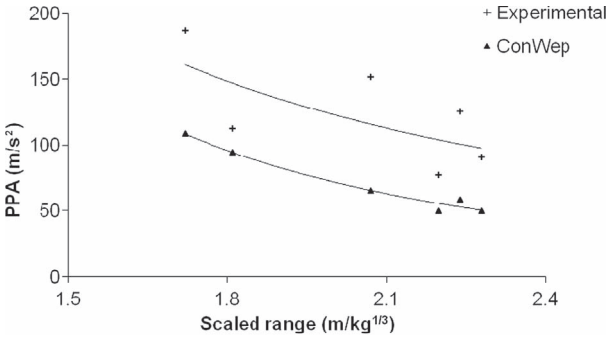

Figure 19. Comparison of peak particle acceleration.

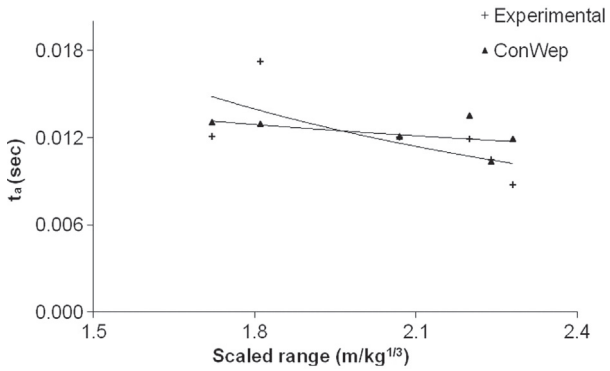

FIGURE 20. Arrival time of ground shock wave.

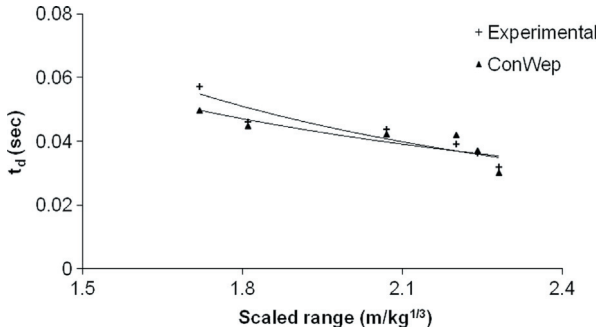

FIGURE 21. Ground shock wave duration.

duration is the difference of total ground shock wave time and time of arrival of ground motions [14]:

$$t_d = T - t_a \quad [14]$$

Empirical formula for shock wave duration [15]:

$$t_d = 0.1308\left(\frac{R}{Q^{1/3}}\right)^{-1.603} \text{ (s)} \quad [15]$$

3.5.4. Time lag between air blast and ground shock wave

Time lag is the difference between arrival time of air blast and ground shock wave.

$T_{lag} = T_a - t_a$

Empirical relationship for T_{lag} [16]:

$$T_{lag} = \frac{8.534}{C_a}\left(\frac{R}{Q^{1/3}}\right)^{-0.996} - \frac{46.17}{C_s}\left(\frac{R}{Q^{1/3}}\right)^{-1.32} \text{ (s)} \quad [16]$$

The time lag between the ground shock and the blast wave shows that the air blast wave reaches the structure before the arrival of ground shocks for small-scaled distances. It was noticed that the time lag is not only related to scaled distance but also to wave propagation velocity in the air and at the site. The values of backfill density, seismic velocity and attenuation coefficient have been assumed on the

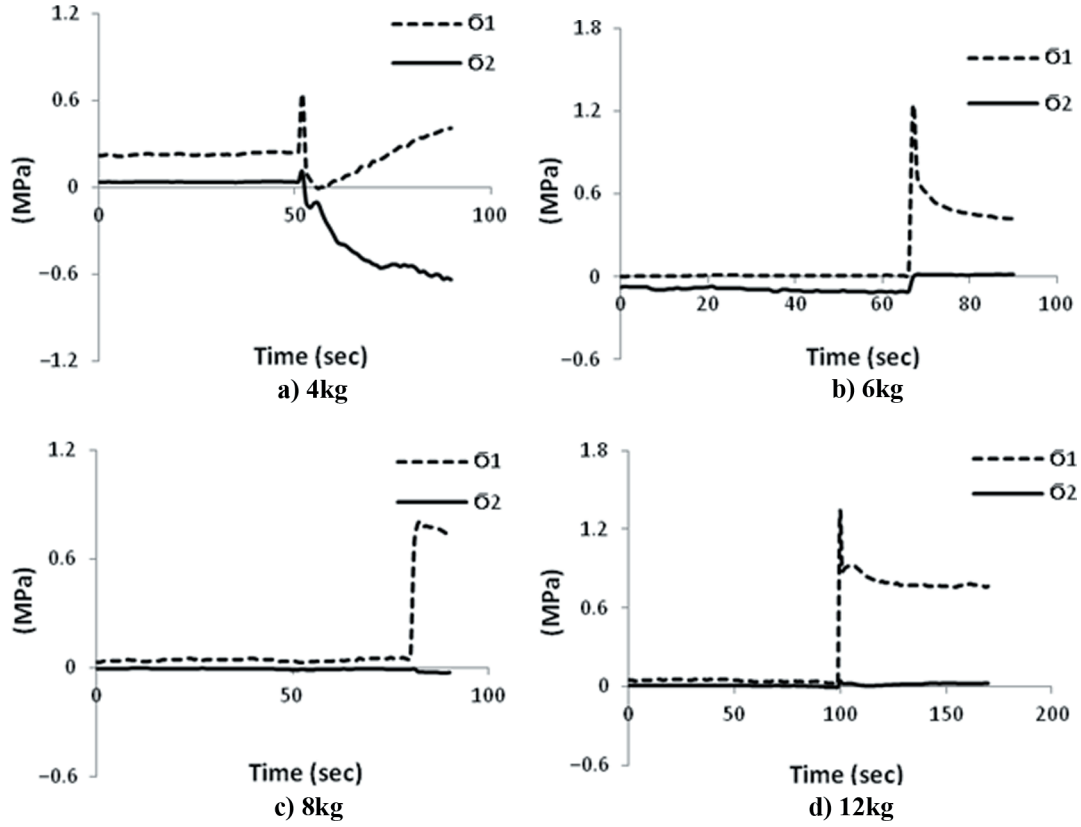

FIGURE 22. Plot of principal stress under explosive loads.

basis of apparent characteristics of soil, which vary with distance and depth. Therefore, it should not be a matter of great concern if the experimental and ConWep results do not match closely.

3.6. Principal stresses

Maximum and minimum principal stress plots of 45° strain rosette for selected element are shown in Figure 22. This figure illustrates stress plots of element, which was directly exposed, to the blast pressure. Principal stress σ_1 for maximum (most tensile) or σ_2 is for minimum (most compressive). As it can be seen that wall is subjected to either tension or compression failure. Wall has completely lost their lost carrying capacity as the principal stresses decreases after blast. Plots of principal stress can be used to find out the damage mechanism and the damage extent for estimation of residual capacity of structures subjected to blast.

4. CONCLUSIONS

The following conclusions are drawn from this study:

- Peak pressure determined by experimental record agrees well with that from Con Wep, design manual, UFC and AASTP chart for hemispherical surface explosion. However, experimental results are comparatively more consistent with those as predicted by AASTP.
- For all scaled distances exponential decay of peak pressure show similar behaviour with previous researchers but quite different at small distance. This is due to difficulty in measuring overpressure at small scaled distances.
- With increasing scaled distance air blast wave arrival time decreases. Also it can be stated that at the same scaled distance, the smaller the explosive weight is, longer will be the arrival time.
- It was noted that the time lag is not only related to scaled distance but also to wave propagation velocity in the air and at the site.
- Consideration of both air blast and ground shock parameters can develop deep understanding of response of structure against explosion.
- For a deeper understanding of response of masonry wall, there is a need for carrying out an extensive experimental work with charge weights of a number of intensities at various standoff distances.

REFERENCES

1. Fischer, K.; Riedel, W.; Ziehm, J. (2011) Full-scale validation of a blast-proof masonry wall system and assessment of coupling effects using a TDOF model. 14th International Symposium on Interaction of the Effects of Munitions with Structures- ISIEMS.
2. Ehsani, M.R.; Saadatmanesh H.; Velazquez-Dimas, J.I. (1999) Behavior of retrofitted URM walls under simulated earthquake loading. *J. Compos. Constr*, 3 [3], 134–142. http://dx.doi.org/10.1061/(ASCE)1090-0268(1999)3:3(134).
3. Varma, R.K.; Tomar, C.P.S.; Parkash, S.; Sethi, V.S. (1996) Damage to brick masonry panel walls under high explosive detonations. ASME-Publications-PVP, 351, 207–216.
4. Casadei, P.; Agneloni, E. (2010) Elastic systems for dynamic retrofitting (ESDR) of structures. 1st International Conference of Protective Structures (ICPS), Manchester, UK.
5. Ward, S.P. (2008) Retrofitting walls to resist blast loads. 20th International Symposium on Military Aspects of Blast and Shock, Oslo, Norway.
6. Wei, X.Y.; Huang, T.; Li, N. (2012) Numerical Derivation of Pressure-Impulse Diagrams for Unreinforced Brick Masonry Walls. *Adv Mater Res Zug*, 368/373, 1435–1439, *4th* International conference Technology of architecture and structure.
7. Wu, C.; Hao, H. (2007) Numerical simulation of structural response and damage to simultaneous ground shock and air blast loads. *Int j impact eng*, 34 [3], 556–572. http://dx.doi.org/10.1016/j.ijimpeng.2005.11.003
8. Godinho, J.; Agnew, E.I.; Marjanishvilli, S. (2007) Resistance of Historic Unreinforced Masonry Walls to Air-Blast Loads. *SO: Structure*, 20–22.
9. Ngo, T.; Mendis, P.; Gupta, A.; Ramsay, J. (2007) Blast loading and blast effects on structures, An overview. *Electron J Struct Eng*, 7, 76–91.
10. Urgessa, G.S.; Maji, A.K. (2009) Dynamic Response of Retrofitted Masonry Walls for Blast Loading. *J Eng Mech*, 136 [7], 858–864. http://dx.doi.org/10.1061/(ASCE)EM.1943-7889.0000128.
11. Wei, X.; Stewart, M.G. (2010) Model validation and parametric study on the blast response of unreinforced brick masonry walls. *Int J Impact Eng*, 37 [11], 1150–1159. http://dx.doi.org/10.1016/j.ijimpeng.2010.04.003.
12. Sorensen, A.; McGill, W.L. (2011) What to look for in the aftermath of an explosion? A review of blast scene damage observables. *Eng Fail Anal*, 18 [3], 836–845. http://dx.doi.org/10.1016/j.engfailanal.2010.12.010.
13. Brode, H.L. (1955) Numerical solutions of spherical blast waves. *J Appl Phys*, 26 [6], 766–775.
14. Henrych, J.; Major, R. (1979) The dynamics of explosion and its use. Elsevier scientific publishing company, New York.
15. Smith, P.D.; Hetherington, J.G. (1994) Blast and ballistic loading of structures. Butterworth-Heinemann Oxford, UK.
16. Formby, S.A.; Wharton, R.K. (1996) Blast characteristics and TNT equivalence values for some commercial explosives detonated at ground level, *J Hazard Mater*, 50 [2], 183–198. http://dx.doi.org/10.1016/0304-3894(96)01791-8.
17. ConWep: Conventional weapons Effects Program. (2005) Version 2.1.0.8 U.S. Army Vicksburg, MS USA.
18. UFC: Structures to Resist the Effects of Accidental Explosions. (2008) Unified Facilities Criteria (UFC) 3-340–02.
19. AASTP: Manual of NATO Safety Principles for the Storage of Military Ammunition and Explosives, (2010). Edition 1, Change 3, Allied Ammunition Storage and Transport Publication.
20. Brode, H.L. (1959) Blast wave from a spherical charge. *Physics of fluids*, 2 [2], 217–229. http://dx.doi.org/10.1063/1.1705911.
21. Brode, H.L. (1968) Review of nuclear weapons effects. *Annual review of nuclear science*, 18 [1], 153–202. http://dx.doi.org/10.1146/annurev.ns.18.120168.001101.
22. Wu, C.; Hao, H. (2005) Modeling of simultaneous ground shock and airblast pressure on nearby structures from surface explosions. *International journal of impact engineering*, 31 [6], 699–717. http://dx.doi.org/10.1016/j.ijimpeng.2004.03.002.
23. Siddiqui, J.I.; Ahmad, S. (2007) Impulsive loading on a concrete structure. Proc. of the Institution of Civil Engineers. Structures and buildings, 160 [4], 231–241. http://dx.doi.org/10.1680/stbu.2007.160.4.231.
24. Ahmad, S.; Elahi, A.; Iqbal, J.; Keyani, M.A.; Rahman, A.G.A. (2012) Impulsive loading on reinforced concrete wall. Proc. of the Institution of Civil Engineers. Structures and buildings. 166 [3], 153–162. http://dx.doi.org/10.1680/stbu.11.00008.